Closure procedure of viscous stress for a non-uniform suspension

Kengo Ichiki[1,2,*] and Andrea Prosperetti[1,2,†]

[1]*Department of Mechanical Engineering, The Johns Hopkins University, Baltimore MD 21218*
[2]*Faculty of Applied Physics, Twente Institute of Mechanics, and Burgerscentrum, University of Twente, AE 7500 Enschede, The Netherlands*

(Dated: March 6, 2004)

It has recently been shown that the average stress in a viscous suspension consists of a symmetric traceless component, and an antisymmetric component expressed in terms of a polar and an axial vector. In this paper, closure relations for these quantities are derived by means of numerical ensemble averaging following a systematic procedure. By the use of a suitably biased probability distribution, the ensemble is made to describe a spatially non-uniform system. Several new terms, which are identically zero for a homogeneous system, are identified. Some interesting artifacts arising from the use of a repeated fundamental cell with the associated artificial periodicity are described.

I. INTRODUCTION

The central problem in the modeling of disperse multiphase flows by means of averaged equations is the closure of the terms which arise from the averaging procedure applied to the exact microscopic equations (see e.g. Refs. 1–4). Such closure requires that part of the information lost upon averaging be reintroduced to a degree of approximation sufficient to capture the physics and result in a well-posed mathematical model.

The problem has been recognized for a long time and many attempts at its solution can be found in the literature. A representative list may include the early paper by Anderson and Jackson[5] dealing with the formulation of a closed model for fluidized beds, the more recent work on the same topic described by Sundaresan[6], work by Koch, Sangani and collaborators devoted to gas-solid suspensions and bubbly liquids (see e.g. Refs. 7–11), the studies by Brady and co-workers on suspension rheology (see e.g. Refs. 12–15), and many others. While the ultimate goal of a general model capable of describing a variety of flow situations is still distant, considerable progress has been achieved by coupling analysis with the detailed computational simulation of flows with suspended particles. With few exceptions (see e.g. Refs. 16,17), most of the work has focused on the limit cases of potential flow (see e.g. Refs. 18–21) and Stokes flow (see e.g. Refs. 22–25), which seem to be the most amenable to the development of a closed model. While idealized, there is hope that the insight gained on these systems might shed useful light for the solution of the problem at intermediate Reynolds numbers.

In some recent papers[26–28] we have considered this problem, again in the Stokes flow limit, pointing out that the information obtainable from the simulation of spatially uniform systems can reflect only partially the full structure of the averaged equations. For example, in a uniform sheared suspension, on average the particles move with the same velocity as the mixture, which does not permit to see the effect of any closure term proportional to the relative velocity of two. Similarly, it is impossible to test the applicability of an effective viscosity calculated from the shear problem to a different flow situation, such as sedimentation, if spatial uniformity causes all spatial gradients to vanish.

To be sure, different flows give rise to different microstructures, which will then have an impact on the effective properties and closure relations (see e.g. Ref. 13). For this reason, the pursuit of a single closed system of averaged equations applicable to many different flow situations may be to some extent futile if a high degree of fidelity is pursued. However, one may look at the general class of problems from another angle. The development of closure relations which, while perhaps not exactly valid for any flow, still manage to capture in some generic sense several important features of many flows, might be a perhaps less ambitious but ultimately, in practice, a more fruitful goal.

It is such a goal which we pursue in this paper and the ones to follow, in which we use spatially periodic ensembles of hard spheres in a cubic fundamental cell to derive in a *systematic* way closure relations for suspensions of equal spheres in Stokes flow. A distinct feature of our approach is the ability to build into this ensemble (by post-processing, as it were) a prescribed spatial non-uniformity in the particle number density distribution.[29,30] In this way, we are able to discern at least some of the effects of non-uniformity alluded to before. One major such effect is the appearance of an antisymmetric component of the stress tensor, entirely due to spatial non-uniformity, even in the absence of couples acting on the particles.

The present paper is devoted to the derivation of a closure relation for the particle stress in the suspension. Future papers will deal with the inter-phase force.

The logic to be followed in these studies is in principle straightforward. Once the fundamental variables of the theory are chosen, considerations of Galilean invariance, parity, linearity, and equipresence dictate the most general form for each closure relation. The quantity to be closed – for example the stress – is calculated directly from its definition by means of numerical ensemble averaging, and so are the quantities appearing in its closure, such as the average rate of strain. Matching the two

requires the introduction of volume-fraction-dependent coefficients – e.g., the effective viscosity – the value of which follows from the direct numerical simulations.

A large fraction of the contemporary work on suspension theory has focused on non-Newtonian rheological properties (see e.g. Refs. 14,31). A great deal of attention has been paid to the anisotropy of the pair distribution function, assuming a spatially homogeneous particle number density. In the present paper we adopt a complementary viewpoint, focusing on non-uniformities of the particle number density while disregarding the anisotropy of the pair distribution function. We believe that our techniques can be extended to deal with the complete problem in which both the particle number density is non-uniform and pair distribution function anisotropic. We will pursue this extension in future work.

II. THE PARTICLE STRESS

We will use as our starting point an expression for the particle stress developed in Ref. 32. That work considered a system of N equal spheres suspended in a fluid in a cubic domain, subjected to periodicity boundary conditions. A closed form expression was obtained for the mean mixture volumetric flux $\boldsymbol{u}_m$ and mixture pressure p_m in terms of ensemble averages of multipole coefficients appearing in Lamb's general solution for the Stokes flow past a sphere[33–35]. The situations considered was fairly general and, in particular, did not assume a spatial homogeneity of the ensemble used to calculate the average. Upon calculating the gradient of p_m and the Laplacian of $\boldsymbol{u}_m$, the following result was found (Eq. (10.3) of Ref. 32):

$$-\boldsymbol{\nabla} p_m + \nabla^2 \boldsymbol{u}_m = -\mu \left[\boldsymbol{\nabla}\cdot \mathsf{S} + \boldsymbol{\nabla}\times(\boldsymbol{R} - \boldsymbol{\nabla}\times\boldsymbol{V})\right] - \frac{1}{v}\int_{|\boldsymbol{r}|\le a} d^3r\, n(\boldsymbol{x}+\boldsymbol{r})\,\overline{\boldsymbol{F}}(\boldsymbol{x}+\boldsymbol{r}) \quad (1)$$

Here S is a traceless symmetric two-tensor, $\boldsymbol{R}$ an axial vector, $\boldsymbol{V}$ a polar vector, n the particle number density, and $\overline{\boldsymbol{F}}$ the average fluid-dynamic force on the particles, each one with radius a and volume $v = \frac{4}{3}\pi a^3$. For a pure fluid with viscosity μ, the right-hand side of this equation would vanish (provided the force is conservative and absorbed in the pressure p_m). The terms in the right-hand side must therefore be identified with the effect of the particles on the momentum balance of the mixture. Starting from the last term, in the absence of inertia, the hydrodynamic force on each particle must balance the applied force. In the case of gravity we therefore have $\overline{\boldsymbol{F}} = v\rho_P \boldsymbol{g}$, with ρ_P the particle density and $\boldsymbol{g}$ the acceleration of gravity, so that the last term of (1) equals $\phi\rho_P\boldsymbol{g}$ in which

$$\phi = \int_{|\boldsymbol{r}|\le a} d^3r\, n(\boldsymbol{x}+\boldsymbol{r}) \quad (2)$$

is the particle volume fraction. This is indeed the expected result for this situation. If we combine the term containing $\boldsymbol{u}_m$ with the remaining terms, we find the divergence of a stress

$$\frac{1}{\mu}\boldsymbol{\Sigma} = 2\mathsf{E}_m + \mathsf{S} + \boldsymbol{\epsilon}\cdot(\boldsymbol{R} - \boldsymbol{\nabla}\times\boldsymbol{V}) \,, \quad (3)$$

in which $\boldsymbol{\epsilon}$ is the alternating tensor and

$$\mathsf{E}_m = \frac{1}{2}\left[\boldsymbol{\nabla}\boldsymbol{u}_m + (\boldsymbol{\nabla}\boldsymbol{u}_m)^\dagger\right] \,, \quad (4)$$

is the mixture rate-of-strain tensor. This expression explicitly shows that the stress tensor contains two anti-symmetric contributions. It is possible to show that, for a uniform suspension,

$$\boldsymbol{R} = \frac{1}{\mu}\overline{\oint_{|\boldsymbol{r}|=a} dS\, \boldsymbol{r}\times[\boldsymbol{\sigma}\cdot\boldsymbol{n}]} \quad (5)$$

where the overline denotes the ensemble average, $\boldsymbol{\sigma}$ is the fluid stress, and $\boldsymbol{n}$ the outwardly directed unit normal at the particle surface. For couple-free particles, this term will therefore vanish. However, additional terms arise in the case of spatial non-uniformities. The term $\boldsymbol{V}$ does not seem to have been identified before. For the spatially uniform case it can be shown to be given by[36]

$$\boldsymbol{V} = -\frac{1}{\mu}\overline{\oint_{|\boldsymbol{r}|=a} dS\, (\mathsf{I} - \boldsymbol{n}\boldsymbol{n})\cdot[\boldsymbol{\sigma}\cdot\boldsymbol{n}]} \,, \quad (6)$$

in which I is the identity two-tensor, and is therefore proportional to the surface-average tangential traction on the particle surface.

As shown in Ref. 32 and summarized in the Appendix, the exact expressions of S, $\boldsymbol{R}$, and $\boldsymbol{V}$ involve an infinite series of multipole coefficients, which reflect the finite size of the particles and therefore, ultimately, the non-local nature of an exact theory. The expressions (5) and (6) are the first terms of the respective infinite series. In this paper we will limit our consideration to the next few terms, which embody a low-order non-local correction. We may also note that, to first order in the particle volume fraction, it is possible to show that

$$\mathsf{S} = 5\phi\mathsf{E}_m \quad (7)$$

so that one recovers the well-known Einstein viscosity correction,[37] and that

$$\boldsymbol{R} = 3\phi\boldsymbol{\Omega}_\Delta, \quad (8)$$

$$\boldsymbol{V} = \frac{3}{10}\phi\,\boldsymbol{u}_\Delta + \frac{1}{7}a^2\mathsf{E}_m\cdot\boldsymbol{\nabla}\phi - \frac{11}{140}\phi a^2\nabla^2\boldsymbol{u}_m, \quad (9)$$

where $\boldsymbol{u}_\Delta = \boldsymbol{U} - \boldsymbol{u}_m$ is the slip translational velocity, defined by the difference between the volumetric flux $\boldsymbol{u}_m$ and the average particle translational velocity $\boldsymbol{U}$, and $\boldsymbol{\Omega}_\Delta = \boldsymbol{\Omega} - (1/2)\boldsymbol{\nabla}\times\boldsymbol{u}_m$ the slip angular velocity. The goal of this paper is to extend these dilute-limit results to the case of finite volume fraction by carrying out numerical ensemble averages.

It may be noted that the contribution of $\boldsymbol{V}$ to the momentum equation in the i-direction may be written identically as

$$-\left(\boldsymbol{\nabla}\times\boldsymbol{\nabla}\times\boldsymbol{V}\right)_i \;=\; \partial_j\left\{\left[\frac{1}{2}\left(\partial_j V_i+\partial_i V_j\right)-\frac{1}{3}\delta_{ij}\boldsymbol{\nabla}\cdot\boldsymbol{V}\right]\right.$$
$$\left.+\frac{1}{2}\left(\partial_j V_i-\partial_i V_j\right)-\frac{2}{3}\delta_{ij}\boldsymbol{\nabla}\cdot\boldsymbol{V}\right\} \qquad (10)$$

in which one recognizes a traceless symmetric term, an antisymmetric term, and an isotropic term. This was the decomposition of the stress adopted in Ref. 27, a study that was carried out before the form (1) of the stress was developed.

III. THE SYMMETRIC PART OF THE STRESS

We assume that the contributions to the stress can be expressed in terms of the local particle volume fraction ϕ, mixture velocity $\boldsymbol{u}_m$, the average inter-phase (or slip) velocity $\boldsymbol{u}_\Delta$, and the average inter-phase angular velocity $\boldsymbol{\Omega}_\Delta$. Since S is a symmetric traceless tensor, if such a representation is possible, it must have the form

$$2\mathsf{E}_m+\mathsf{S}=2\mu_e\mathsf{E}_m+2\mu_\Delta\mathsf{E}_\Delta+2\mu_\nabla\mathsf{E}_\nabla+2\mu_\Omega\mathsf{E}_\Omega$$
$$+a^2\left(\mu_0\nabla^2\mathsf{E}_m+\mu_1\mathsf{E}_m\nabla^2\phi\right)+\ldots \qquad (11)$$

where E_Δ, E_∇ and E_Ω are defined respectively by

$$\mathsf{E}_\Delta \;=\; \frac{1}{2}\left[\boldsymbol{\nabla}\boldsymbol{u}_\Delta+\left(\boldsymbol{\nabla}\boldsymbol{u}_\Delta\right)^\dagger\right]-\frac{1}{3}\left(\boldsymbol{\nabla}\cdot\boldsymbol{u}_\Delta\right)\mathsf{I}, \qquad (12)$$
$$\mathsf{E}_\nabla \;=\; \frac{1}{2}\left[\boldsymbol{u}_\Delta\boldsymbol{\nabla}\phi+\left(\boldsymbol{u}_\Delta\boldsymbol{\nabla}\phi\right)^\dagger\right]-\frac{1}{3}\left(\boldsymbol{u}_\Delta\cdot\boldsymbol{\nabla}\phi\right)\mathsf{I}, \qquad (13)$$
$$\mathsf{E}_\Omega \;=\; \frac{1}{2}\left\{\left[\boldsymbol{\nabla}\left(\boldsymbol{\nabla}\times\boldsymbol{\Omega}_\Delta\right)\right]+\left[\boldsymbol{\nabla}\left(\boldsymbol{\nabla}\times\boldsymbol{\Omega}_\Delta\right)\right]^\dagger\right\}, \qquad (14)$$

in which μ_e is the usual effective viscosity (normalized by the viscosity of the suspending fluid), while the other μ's are additional viscosity parameters. The reason for exhibiting the terms shown in (11) disregarding, for example, a term proportional to $\nabla^2\mathsf{E}_\Delta$ and similar ones (denoted by the dots in the equation) will be clarified later, after Eq. (40).

We now apply to the present closure problem the same techniques developed earlier in Refs. 26,27,29. The method is described in detail in these references and a brief summary will be sufficient here. We construct a homogeneous ensemble of hard-sphere configurations by placing N particles in a cubic box of side L and subjecting them to random displacements. For each value of the volume fraction, we construct in this way several ensembles containing between 10 and 160 spheres, and between 256 and 2048 configurations (see Ref. 29 for details). While a direct averaging would produce ensemble averages corresponding to a spatially homogeneous system, by suitably biasing the uniform-system probability, we produce results which correspond to a non-uniform number density distribution

$$n(\boldsymbol{x}) \;=\; n_0\left(1+\epsilon\sin\boldsymbol{k}\cdot\boldsymbol{x}\right) \qquad (15)$$

in which $n_0=N/L^3$, $\boldsymbol{k}$ is a vector with modulus $2\pi/L$ parallel to one of the sides of the box, and ϵ a small parameter. As a result of this procedure all the average quantities will consist of a constant part and a sinusoidal (or co-sinusoidal) disturbance. The introduction of the parameter ϵ enables us to identify unequivocally the latter part above the statistical noise. The use of ensembles with a different number of particles for the same volume fraction enables us to vary the box side L and, therefore, $\boldsymbol{k}$.

For each configuration of the ensemble, we subject the particles to an equal force $\boldsymbol{F}_0$, directed parallel to the sides of the box, and calculate the resulting linear and angular velocity of each. We refer to this as the force problem and we attach an index F to the quantities related to it. The results are averaged as explained before and, for example for the case of the slip velocity, parameterized as

$$\boldsymbol{u}_\Delta(\boldsymbol{x}) \;=\; \left[u_\Delta\right]_F^0\boldsymbol{W}_F$$
$$+\;\epsilon\sin\left(\boldsymbol{k}\cdot\boldsymbol{x}\right)\left(\left[u_\Delta\right]_F^{\parallel}\boldsymbol{W}_F^{\parallel}+\left[u_\Delta\right]_F^{\perp}\boldsymbol{W}_F^{\perp}\right) \qquad (16)$$

Here

$$\boldsymbol{W}_F \;=\; \frac{\boldsymbol{F}_0}{6\pi\mu a} \qquad (17)$$

is the sedimentation velocity of a single isolated particle and represents the fundamental vector characterizing this problem. The vectors $\boldsymbol{W}_F^{\parallel}$ and $\boldsymbol{W}_F^{\perp}$ are its projection parallel and orthogonal to the non-uniformity vector $\boldsymbol{k}$. The coefficients of a term proportional to $\cos\left(\boldsymbol{k}\cdot\boldsymbol{x}\right)$ are found to vanish. The symbol $\left[u_\Delta\right]_F^0$ represents the numerically calculated average sedimentation velocity corresponding to the uniform particle number density n_0, while $\left[u_\Delta\right]_F^{\parallel}$ and $\left[u_\Delta\right]_F^{\perp}$ represent the effect of the spatially non-uniform part of the number density. These coefficients depend on both the wave vector k and the volume fraction ϕ. The volumetric flux $\boldsymbol{u}_m$ is parameterized in a similar way, except that all the parallel coefficients vanish due to incompressibility.

We proceed in a similar fashion subjecting each particle to an equal couple $\boldsymbol{T}_0$, directed parallel to the sides of the box, again calculating the resulting linear and angular velocities (torque problem, index T). For this problem, the polar vector playing a role analogous to $\boldsymbol{W}_F$ is

$$\boldsymbol{W}_T^{\perp} \;=\; a\hat{\boldsymbol{k}}\times\frac{\boldsymbol{T}_0}{8\pi\mu a^3}\,, \qquad (18)$$

where $\hat{\boldsymbol{k}}=\boldsymbol{k}/k$, with $k=|\boldsymbol{k}|$. The parameterization of the numerical ensemble averages is expressed similarly to (16), but only the coefficient $\left[u_\Delta\right]_T^{\perp}$ of the cosine term is found to be non-zero.

Finally, we write the fluid velocity as the sum of an imposed deterministic uniform shear field $\boldsymbol{u}^\infty(\boldsymbol{x})=\mathsf{E}^\infty\cdot\boldsymbol{x}$ and a periodic disturbance due to the particles and, again, calculate the resulting linear and angular velocity

of each particle (shear problem, index E). In this case there is no fundamental vector analogous to $\boldsymbol{W}_F$, but one can define two vectors playing the role of $\boldsymbol{W}_F^{\parallel}$ and $\boldsymbol{W}_F^{\perp}$, namely

$$\boldsymbol{W}_E^{\parallel} = a\left(\hat{\boldsymbol{k}}\hat{\boldsymbol{k}}\right)\cdot\left(\mathsf{E}^{\infty}\cdot\hat{\boldsymbol{k}}\right), \tag{19}$$

$$\boldsymbol{W}_E^{\perp} = a\left(\mathsf{I}-\hat{\boldsymbol{k}}\hat{\boldsymbol{k}}\right)\cdot\left(\mathsf{E}^{\infty}\cdot\hat{\boldsymbol{k}}\right), \tag{20}$$

Both coefficients $[u_\Delta]_E^{\perp}$ and $[u_\Delta]_E^{\parallel}$ of the cosine term are found to be non-zero.

From the representations (16) of $\boldsymbol{u}_\Delta$ and the analogous ones for $\boldsymbol{u}_m$ for the three physical situations, one can calculate the tensors appearing in the right-hand side of (11) finding linear combinations of E^{∞} and the two tensors

$$\mathsf{G}^{\perp} = \boldsymbol{W}^{\perp}\hat{\boldsymbol{k}}+\hat{\boldsymbol{k}}\boldsymbol{W}^{\perp}, \tag{21}$$

$$\mathsf{G}^{\parallel} = \frac{1}{2}\left(\boldsymbol{W}^{\parallel}\hat{\boldsymbol{k}}+\hat{\boldsymbol{k}}\boldsymbol{W}^{\parallel}\right)-\frac{1}{3}\left(\hat{\boldsymbol{k}}\cdot\boldsymbol{W}^{\parallel}\right)\mathsf{I}, \tag{22}$$

where each vector $\boldsymbol{W}$ carries the appropriate index F, T, or E.

The symmetric stress S can also be calculated from the results of the numerical simulations using its expression (A.1) in terms of multipole coefficients and the results parameterized in a similar fashion. For example, for the shear problem, we find

$$\begin{aligned}\mathsf{S}(\boldsymbol{x}) &= [S]_E^0\mathsf{E}^{\infty} \\ &+ \epsilon\sin(\boldsymbol{k}\cdot\boldsymbol{x})\left([S]_E^E\mathsf{E}^{\infty}+[S]_E^{\perp}\mathsf{G}_E^{\perp}+[S]_E^{\parallel}\mathsf{G}_E^{\parallel}\right),\end{aligned} \tag{23}$$

where, again, the coefficients $[S]_E^0$, $[S]_E^E$, $[S]_E^{\perp}$, and $[S]_E^{\parallel}$ depend on both the wave vector k and the volume fraction ϕ.

The same procedure is followed for the force and the torque problems. In the case of the former, only the coefficients $[S]_F^{\perp}$ and $[S]_F^{\parallel}$ of the cosine are non-zero while, for the latter, only the coefficient $[S]_T^{\perp}$ of the sine is non-zero.

At this point, both sides of the closure relation (11) have the form of a linear combination of the tensors E^{∞}, $\mathsf{G}^{\perp}$, and $\mathsf{G}^{\parallel}$. Upon equating the coefficients of each one of these tensors in the two sides, we find

$$[S]_E^0 = 2\left(\mu_e-1\right) \tag{24}$$

$$[S]_E^E = 2\phi\left\{\frac{\mathrm{d}\mu_e}{\mathrm{d}\phi}-\left(\frac{1}{10}\frac{\mathrm{d}\mu_e}{\mathrm{d}\phi}+\mu_1\right)(ka)^2\right\}, \tag{25}$$

$$\frac{[S]_E^{\parallel}}{2} = -\mu_\Delta ka[u_\Delta]_E^{\parallel}, \tag{26}$$

$$\begin{aligned}[S]_E^{\perp} &= -\left\{\mu_e-1-(ka)^2\mu_0\right\}ka[u_m]_E^{\perp}-\mu_\Delta ka[u_\Delta]_E^{\perp} \\ &\quad +\mu_\Omega(ka)^2[\Omega_\Delta]_E^{\perp},\end{aligned} \tag{27}$$

$$\begin{aligned}[S]_T^{\perp} &= -\left\{\mu_e-1-(ka)^2\mu_0\right\}ka[u_m]_T^{\perp}-\mu_\Delta ka[u_\Delta]_T^{\perp} \\ &\quad -\mu_\Omega(ka)^2[\Omega_\Delta]_T^{\perp},\end{aligned} \tag{28}$$

$$\frac{[S]_F^{\parallel}}{2} = \mu_\Delta ka[u_\Delta]_F^{\parallel}+\mu_\nabla\phi ka[u_\Delta]_F^0, \tag{29}$$

$$\begin{aligned}[S]_F^{\perp} &= \left\{\mu_e-1-(ka)^2\mu_0\right\}ka[u_m]_F^{\perp}+\mu_\Delta ka[u_\Delta]_F^{\perp} \\ &\quad +\mu_\nabla\phi ka[u_\Delta]_F^0+\mu_\Omega(ka)^2[\Omega_\Delta]_F^{\perp}.\end{aligned} \tag{30}$$

The second relation (25) arises from the fact that, since $\phi'=\phi(1+\epsilon\sin\boldsymbol{k}\cdot\boldsymbol{x})$ (see Eq. 15), and since $\mu_e=\mu_e(\phi)$, we have

$$\mu_e(\phi')=\mu_e(\phi')+(\phi'-\phi)\frac{\mathrm{d}\mu_e}{\mathrm{d}\phi}. \tag{31}$$

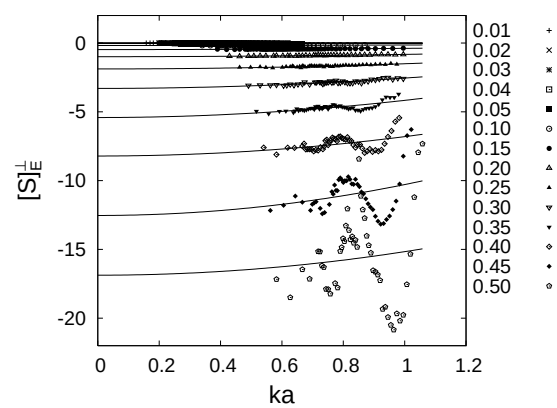

FIG. 1: An example of the k-dependence of the average coefficients appearing in Eq. (24) for $[S]_E^{\perp}$. This is the same coefficient shown in Fig. 1 of Ref. 27. Other examples can be found in Ref. 29.

As noted above, the use of boxes with different sides L for the same volume fraction enables us to find the dependence of the various coefficients on the wavenumber k for a given volume fraction. A typical example for the case of the coefficient $[S]_E^{\perp}$ is shown in Fig. 1. An interesting feature of these results, as well as the similar ones for the other coefficients appearing in (33) to (35), is the presence of stronger oscillations as the volume fraction is increased. Some comments on this point are given later.

As in our earlier paper, Ref. 29, these and the analogous numerical results for the other coefficients are then

fitted as functions of ka as

$$[S]_E^0 = D^{[S]_E^0}, \quad (32)$$
$$[S]_E^E = D^{[S]_E^E} + (ka)^2 A^{[S]_E^E}, \quad (33)$$
$$[S]_E^{\parallel} = 0 + (ka)^2 A^{[S]_E^{\parallel}}, \quad (34)$$
$$[S]_E^{\perp} = D^{[S]_E^{\perp}} + (ka)^2 A^{[S]_E^{\perp}}, \quad (35)$$
$$[S]_T^{\perp} = D^{[S]_T^{\perp}} + (ka)^2 A^{[S]_T^{\perp}}, \quad (36)$$
$$[S]_F^{\parallel} = \frac{1}{ka}\left(0 + (ka)^2 A^{[S]_F^{\parallel}} + (ka)^3 B^{[S]_F^{\parallel}}\right), \quad (37)$$
$$[S]_F^{\perp} = \frac{1}{ka}\left(D^{[S]_F^{\perp}} + (ka)^2 A^{[S]_F^{\perp}} + (ka)^3 B^{[S]_F^{\perp}}\right), \quad (38)$$

in which the coefficients A, B, and D are the product of the fitting procedure. Similar fits are generated for the k-dependence of the coefficients of $\boldsymbol{u}_m$, $\boldsymbol{u}_\Delta$. For example, for the force problem,

$$[u_m]_F^{\perp} = \frac{1}{k^2}\left(D^{[u_m]_F^{\perp}} + k^2 A^{[u_m]_F^{\perp}} + k^3 B^{[u_m]_F^{\perp}}\right) \quad (39)$$
$$[u_\Delta]_F^{\perp} = A^{[u_\Delta]_F^{\perp}} + kB^{[u_\Delta]_F^{\perp}} \quad (40)$$

The other fits, from our earlier paper,[29] are shown in the Appendix. It is seen from these expressions that E_m is $O(k^{-2})$ with respect to E_Δ, E_∇, and E_Ω as $k \to 0$. The terms shown in Eq. (11), therefore, are sufficient to include the two leading terms in k, as $k \to 0$, for the three physical situations considered in this paper.

A. The effective viscosity

When the fits (32) to (38) and the similar ones for $\boldsymbol{u}_m$, $\boldsymbol{u}_\Delta$ are substituted into the relations (24) to (30) and the coefficients of corresponding powers of k equated, to leading order (i.e., to k^0 for the shear problem and k^{-1} for force and torque problems) we find several alternative expressions for the effective viscosity:

$$\mu_e = 1 + \frac{1}{2}D^{[S]_E^0} = 1 + \lim_{k\to 0}\frac{[S]_E^0}{2}, \quad (41)$$
$$\frac{\mathrm{d}\mu_e}{\mathrm{d}\phi} = \frac{1}{2\phi}D^{[S]_E^E} = \lim_{k\to 0}\frac{[S]_E^E}{2\phi}, \quad (42)$$
$$\mu_e = 1 - \frac{D^{[S]_E^{\perp}}}{D^{[u_m]_E^{\perp}}} = 1 - \lim_{k\to 0}\frac{[S]_E^{\perp}}{k[u_m]_E^{\perp}}, \quad (43)$$
$$\mu_e = 1 - \frac{D^{[S]_T^{\perp}}}{D^{[u_m]_T^{\perp}}} = 1 - \lim_{k\to 0}\frac{[S]_T^{\perp}}{k[u_m]_T^{\perp}}, \quad (44)$$
$$\mu_e = 1 + \frac{D^{[S]_F^{\perp}}}{D^{[u_m]_F^{\perp}}} = 1 + \lim_{k\to 0}\frac{[S]_F^{\perp}}{k[u_m]_F^{\perp}}. \quad (45)$$

Consistency among these results would imply that μ_e is a robust quantity which has the same value in three very different physical situations.

An excellent consistency can indeed be observed in Fig. 2, which shows μ_e calculated from the uniform part of the shear problem (open squares, Eq. 41), and from the non-uniform parts of the shear problem (open circles, Eq. 43), of the torque problem (up-triangles, Eq. 44), and of the force problem (down-triangles, Eq. 45).

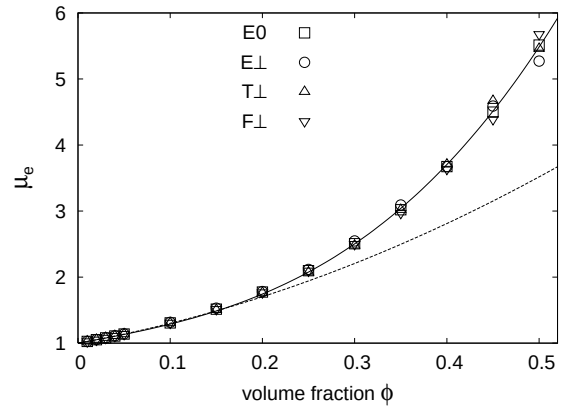

FIG. 2: μ_e from (41), (43), (44) and (45). Dashed and solid lines show the dilute-limit fit (46) and the whole-range fit $(5/2)\phi + A\phi^2 + B\phi^3$.

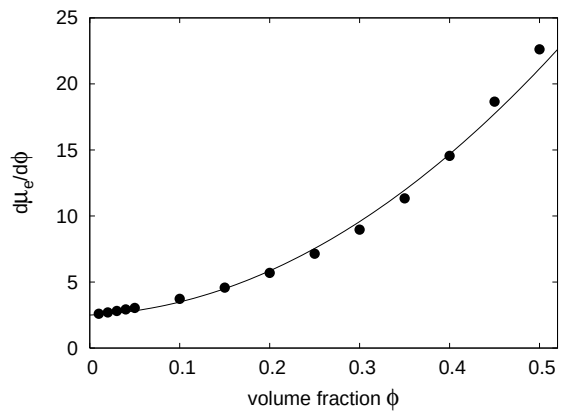

FIG. 3: $\mathrm{d}\mu_e/\mathrm{d}\phi$ from (42). The solid line is the derivative of the whole-range fit of μ_e given in the text.

For $\phi \leq 0.05$, μ_e is well fitted by

$$\mu_e = 1 + \frac{5}{2}\phi + 5.07\phi^2. \quad (46)$$

As mentioned before, the present calculations are done with the assumption of an isotropic two-body correlation function including multipoles up to the fifth order. It is well known that the coefficient of the ϕ^2 term depends on the multipole truncation,[38] as well as the microstructure, such as the anisotropy of the pair distribution function.[39] Our result 5.07 for this coefficient is consistent with earlier studies, such as 5.2 by Batchelor and Green[40] with all moments, and 4.84 by Beenakker[38] obtained by means of a concentration expansion. Over the whole range of ϕ, our numerical result for μ_e is well fitted by $\mu_e = 1 + 2.5\phi + A\phi^2 + B\phi^3$, with $A = 1.52$ and $B = 22.8$ as shown by the solid line in Fig. 2.

Since in our calculation we only include multipoles up

to the fifth order without lubrication corrections, the accuracy of our results decreases with increasing ϕ. For example, for $\phi = 25\%$ and 45%, we find $\mu_e = 2.10$ and 4.5, respectively, as shown in Table I, to be compared with (about) 2.17 and 5.6 as reported by Ladd.[41]

A further consistency test is offered by comparing Eq. (42) for $d\mu_e/d\phi$ with the derivative calculated from the fitting as $\mathrm{d}\mu_e/\mathrm{d}\phi = 2.5 + 2A\phi + 3B\phi^2$ shown in Fig. 3. The observed consistency implies that, for weak spatial non-uniformity (as measured by ϵ, cf. Eq. 15), the effective viscosity only depends on the local value of the volume fraction.

TABLE I: Closure coefficient μ_e.

ϕ	$E0$	$E\perp$	$T\perp$	$F\perp$
0.01	1.02548	1.025	1.025	1.0257
0.02	1.05196	1.051	1.052	1.0522
0.03	1.07947	1.079	1.080	1.0796
0.04	1.10810	1.108	1.109	1.1078
0.05	1.13788	1.138	1.137	1.1371
0.10	1.3063	1.312	1.305	1.300
0.15	1.5145	1.53	1.505	1.496
0.20	1.773	1.79	1.76	1.742
0.25	2.098	2.12	2.07	2.05
0.30	2.505	2.52	2.47	2.44
0.35	3.021	3.0	3.0	2.94
0.40	3.673	3.7	3.7	3.55
0.45	4.50	4.5	4.6	4.3
0.50	5.51	5.4	5.4	5.3

B. Behavior of the coefficients

In principle, by applying the same matching procedure used to obtain Eqs. (41) to (45) to the terms proportional to higher powers of k, one should be able to determine the additional viscosity parameters μ_Δ and μ_∇, and μ_Ω appearing in the closure relation (11). We have however encountered some difficulties in following this path.

In the first place, from the results of the least-squares fitting, one may deduce that the accuracy with which the higher-order coefficients in relations such as (33) to (38) can be determined is lower than that of the leading terms. One cause of this lower accuracy is the statistical error inherent in the averaging procedure. Since the lowest-order coefficient carries the bulk of the numerical information, this statistical error magnifies the relative error affecting the higher-order coefficients.

Secondly, the k-dependence of the physical quantities in general is not well understood. For example, even for as simple a quantity as the sedimentation velocity, we have found[29] that the effect of the imposed periodicity deriving from the use of a fundamental cell is not well described by the existing models.

Another consequence of the artificial periodicity appears to be the oscillatory k-behavior observed in Fig. 1, which is encountered in the case of other coefficients of S

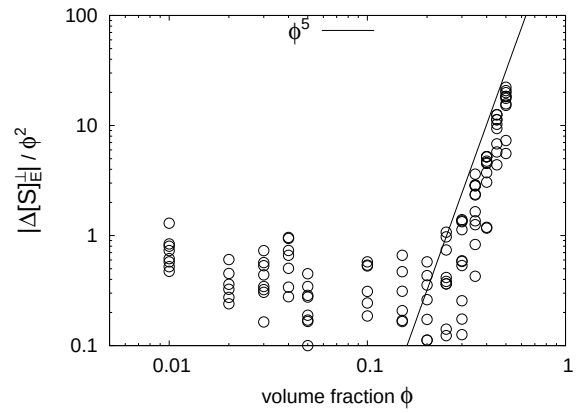

FIG. 4: Amplitudes of the oscillations of $|\Delta\,[S]_E^\perp\,|/\phi^2$ for $N = 30$ to 40 versus volume fraction ϕ. At the higher concentrations, this quantity is found to scale approximately as ϕ^5.

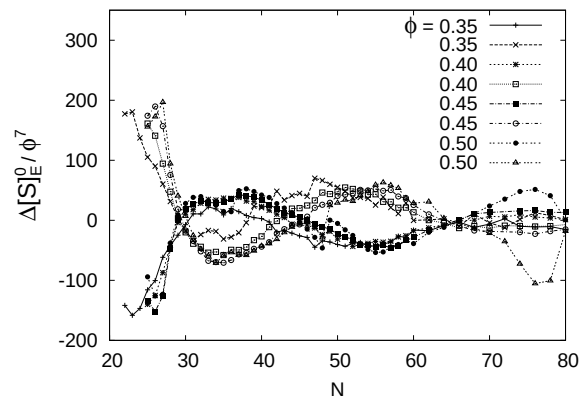

FIG. 5: Numerical results for $[S]_E^0$ grouped separately for the extensional (positive value for small N) and shear flows scaled by ϕ^7 vs. N.

as well. To study this point, we extract the oscillations subtracting the fitted forms as, for example,

$$\Delta\,[S]_E^\perp = [S]_E^\perp - \left(D^{[S]_E^\perp} + k^2 A^{[S]_E^\perp}\right). \qquad (47)$$

Figure 4 shows the absolute value of the oscillations $|\Delta\,[S]_E^\perp\,|$ divided by ϕ^2 in the range $30 \le N \le 40$ where, as Figs. 5 to 7 show, a peak of the oscillation appears. The factor ϕ^2 comes from the fact that, numerically, $D^{[S]_E^\perp} = -13.0\phi^2 + O(\phi^3)$. The amplitude of the oscillations is particularly prominent at the higher densities.

For the shear problem, the effective viscosity is essentially the coefficient $[S]_E^0$ which is obtained from the uniform average without introducing the statistical bias which produces the non-uniform number density given in (15). If, in calculating this quantity, we separate the average found for the cases of extensional flow (diagonal E^∞) from those for shear flow (in which E^∞ has only off-diagonal elements), we find results that oscillate about each other as shown in Fig. 5. When these two averages

are combined to produce the final average, however, the oscillations disappear and this quantity becomes almost independent of k. This result may be related to the fact that, when the particles are arranged in a regular simple cubic lattice, there are two different values of the effective viscosity.[42]

The numerical results for $\Delta\left[S\right]_E^{\perp}$ are shown in Fig. 6 scaled by ϕ^7. With this scaling, the results are found to be nearly independent of ϕ and to exhibit a strong regularity in their dependence on the number of particles in the unit cell, rather than on ka. Indeed, upon comparing Figs. 4 and 6, we notice that the zeros cluster around the interesting numbers $N = 27(= 3^3)$, $45(= 2^2 3^3)$, and $64(= 4^3)$. A similar behavior is encountered for all the other $\Delta\left[S\right]$ quantities, which are scaled in the same way and shown together in Fig. 7 for $\phi = 45\%$.

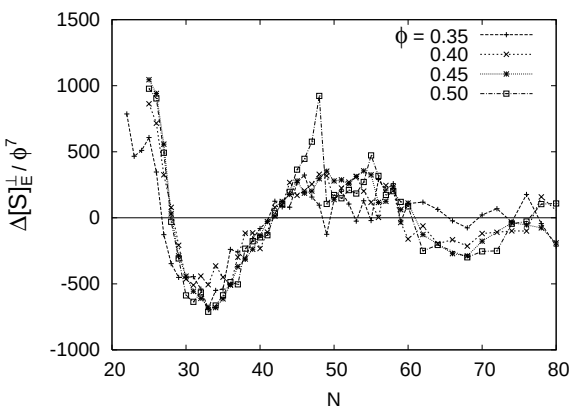

FIG. 6: $\Delta\left[S\right]_E^{\perp}/\phi^7$ vs. N for different volume fractions.

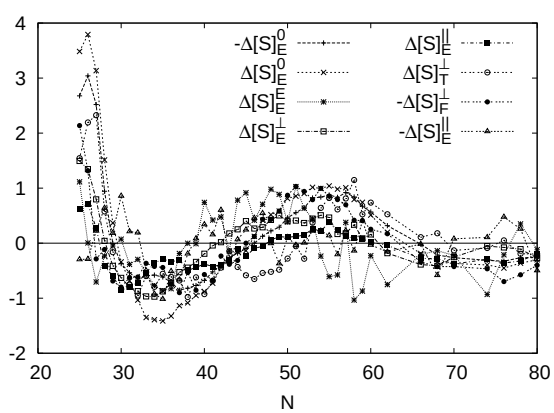

FIG. 7: $\Delta\left[S\right]/\phi^7$ vs. N for $\phi = 0.45$ and all cases.

The observed regularity of the oscillatory behavior that we have described suggests the presence of a well-defined mechanism which is not a statistical artifact.

IV. THE POLAR VECTOR OF THE ANTISYMMETRIC STRESS

We proceed in the same way for the polar vector of the antisymmetric stress, $\boldsymbol{V}$. By including all the terms with the correct parity and vectorial nature which contribute to leading order in k we write

$$\begin{aligned}\boldsymbol{V} &= V_1\boldsymbol{u}_\Delta \\ &\quad +V_2 a^2 \mathsf{E}_m\cdot\boldsymbol{\nabla}\phi + V_3 a^2\nabla^2\boldsymbol{u}_m \\ &\quad +a^2\boldsymbol{\nabla}\times\left(V_\Omega\boldsymbol{\Omega}_\Delta\right). \end{aligned} \tag{48}$$

We should note that, writing the last term in the form shown rather than, more generally, as a linear combination of $\boldsymbol{\nabla}\times\boldsymbol{\Omega}_\Delta$ and $\boldsymbol{\Omega}_\Delta\times\boldsymbol{\nabla}\phi$, is an educated guess the accuracy of which we have no way to assess.

The leading terms in k give

$$[V]_F^0 = V_1[u_\Delta]_F^0, \tag{49}$$

$$[V]_F^{\parallel} = V_1[u_\Delta]_F^{\parallel} + \phi\frac{\mathrm{d}V_1}{\mathrm{d}\phi}[u_\Delta]_F^0, \tag{50}$$

$$[V]_F^{\perp} = V_1[u_\Delta]_F^{\perp} + \phi\frac{\mathrm{d}V_1}{\mathrm{d}\phi}[u_\Delta]_F^0 - V_3(ka)^2[u_m]_F^{\perp}, \tag{51}$$

$$\begin{aligned}[V]_T^{\perp} &= V_1[u_\Delta]_T^{\perp} - V_3(ka)^2[u_m]_T^{\perp} \\ &\quad +\phi\frac{\mathrm{d}}{\mathrm{d}\phi}\left(V_\Omega\,\Omega\right),\end{aligned} \tag{52}$$

$$[V]_E^{\parallel} = V_1[u_\Delta]_E^{\parallel} + V_2 ka\phi, \tag{53}$$

$$[V]_E^{\perp} = V_1[u_\Delta]_E^{\perp} - V_3 k^2[u_m]_E^{\perp} + V_2 ka\phi. \tag{54}$$

Here $\Omega(\phi)$ is the hindrance function for rotation introduced later in Eq. (67). Terms of higher-order in k are shown in the Appendix.

The coefficient V_1 is determined from the uniform part of the force problem as

$$V_1 = \frac{A^{[V]_F^0}}{A^{[u_\Delta]_F^0}}, \tag{55}$$

which is the limit of (49) as $k\to 0$. Figure 8 shows this coefficient calculated from (55). It is seen that V_1 increases rapidly with concentration, which makes the effect of the corresponding term significant for non-dilute suspensions.

Substituting V_1 from (55) into (50) and taking the limit $k\to 0$, we have $\phi\ \mathrm{d}V_1/\mathrm{d}\phi$ from the parallel component of the force problem as

$$\phi\frac{\mathrm{d}V_1}{\mathrm{d}\phi} = \frac{1}{A^{[u_\Delta]_F^0}}\left(A^{[V]_F^{\parallel}} - A^{[V]_F^0}\frac{A^{[u_\Delta]_F^{\parallel}}}{A^{[u_\Delta]_F^0}}\right). \tag{56}$$

Figure 9 shows $\mathrm{d}V_1/\mathrm{d}\phi$ calculated from (56), as well as the estimation by numerical differentiation of (55). The two results are consistent.

From the perpendicular component of the force prob-

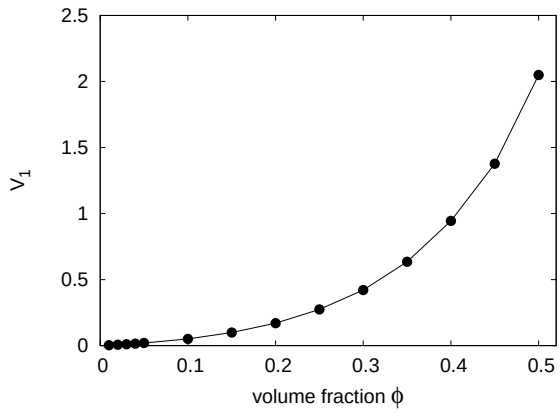

FIG. 8: The coefficient V_1 introduced in Eq. (48) and calculated from (55) vs. volume fraction ϕ.

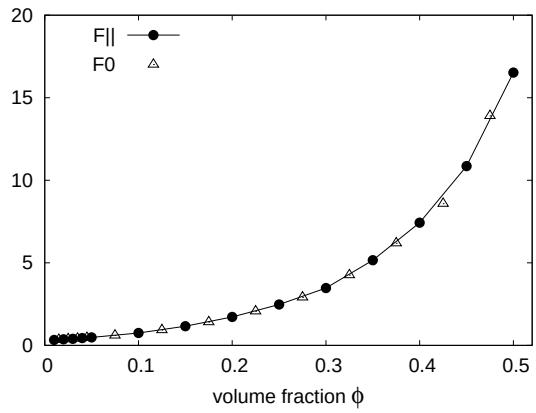

FIG. 9: Derivative $\mathrm{d}V_1/\mathrm{d}\phi$ of the coefficient V_1 from (56) (circles) compared with the numerical differentiation of the results of the previous figure (triangles).

lem (51), we have V_3 as

$$V_3(\phi) = \frac{1}{D^{[u_m]_F^\perp}} \left(A^{[V]_F^\parallel} - A^{[V]_F^\perp} - A^{[V]_F^0} \frac{A^{[u_\Delta]_F^\parallel} - A^{[u_\Delta]_F^\perp}}{A^{[u_\Delta]_F^0}} \right). \quad (57)$$

From the parallel component of the shear problem (53), we have V_2 as

$$V_2(\phi) = \frac{1}{\phi} \left(A^{[V]_E^\parallel} - A^{[V]_F^0} \frac{A^{[u_\Delta]_E^\parallel}}{A^{[u_\Delta]_F^0}} \right), \quad (58)$$

which, substituted into the perpendicular component of the shear problem (54), gives an alternative expression for V_3:

$$V_3(\phi) = \frac{1}{D^{[u_m]_E^\perp}} \left(A^{[V]_E^\parallel} - A^{[V]_E^\perp} - A^{[V]_F^0} \frac{A^{[u_\Delta]_E^\parallel} - A^{[u_\Delta]_E^\perp}}{A^{[u_\Delta]_F^0}} \right). \quad (59)$$

Figure 10 shows V_3/ϕ calculated from (57) and (59). Division by ϕ is suggested by the dilute-limit result (9) which predicts a value -11/140 for this quantity (horizontal line) as $\phi \to 0$, in good agreement with the numerical results. The consistency between the two determinations of V_3 is also good, which implies, among others, that V_1 calculated for the torque and shear problems is consistent with that calculated for the force problem.

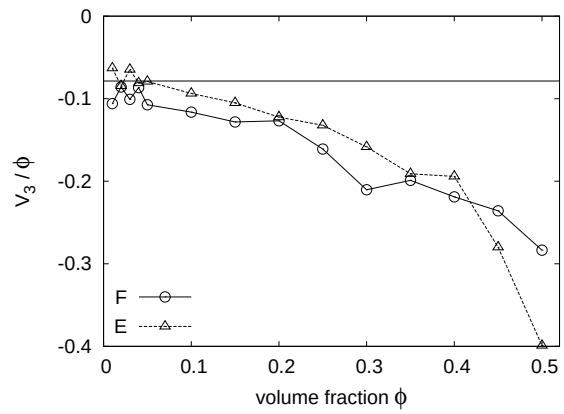

FIG. 10: Graph of V_3/ϕ compared with the dilute-limit result -11/140 shown by the horizontal line.

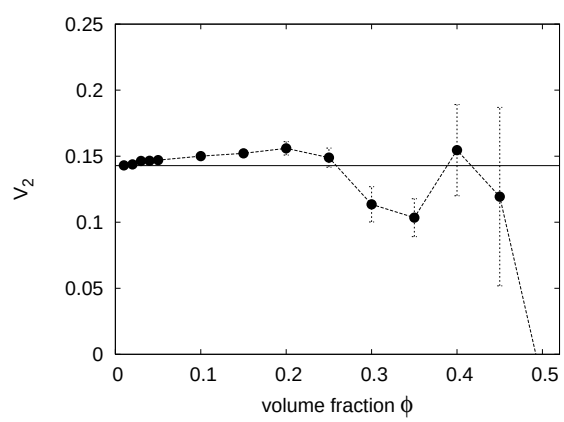

FIG. 11: The coefficient V_2; the solid line is the dilute-limit result 1/7.

Figure 11 shows V_2 calculated from (58). The horizontal line is the value 1/7 given by the dilute result (9), with which the numerical results are in close agreement. For volume fractions of 30% and higher, the error is larger and it is difficult to make definite statements on the ϕ-dependence of this quantity in this range.

From (52), upon using (57) to express V_3, we have

$$\phi\frac{\mathrm{d}}{\mathrm{d}\phi}\left(V_\Omega\ \Omega\right) = A^{[V]^\perp_T} - V_1 A^{[u_\Delta]^\perp_T} + V_3 D^{[u_m]^\perp_T} \quad (60)$$

$$= A^{[V]^\perp_T} + \frac{D^{[u_m]^\perp_T}}{D^{[u_m]^\perp_F}}\left(A^{[V]^\parallel_F} - A^{[V]^\perp_F}\right) \quad (61)$$

$$-\frac{A^{[V]^0_F}}{A^{[u_\Delta]^0_F}}\left\{A^{[u_\Delta]^\perp_T} + \frac{D^{[u_m]^\perp_T}}{D^{[u_m]^\perp_F}}\left(A^{[u_\Delta]^\parallel_F} - A^{[u_\Delta]^\perp_F}\right)\right\},$$

or, alternatively, upon using (59),

$$\phi\frac{\mathrm{d}}{\mathrm{d}\phi}\left(V_\Omega\ \Omega\right) = A^{[V]^\perp_T} + \frac{D^{[u_m]^\perp_T}}{D^{[u_m]^\perp_E}}\left(A^{[V]^\parallel_E} - A^{[V]^\perp_E}\right)$$

$$-\frac{A^{[V]^0_E}}{A^{[u_\Delta]^0_E}}\left\{A^{[u_\Delta]^\perp_T} + \frac{D^{[u_m]^\perp_T}}{D^{[u_m]^\perp_E}}\left(A^{[u_\Delta]^\parallel_E} - A^{[u_\Delta]^\perp_E}\right)\right\}, \quad (62)$$

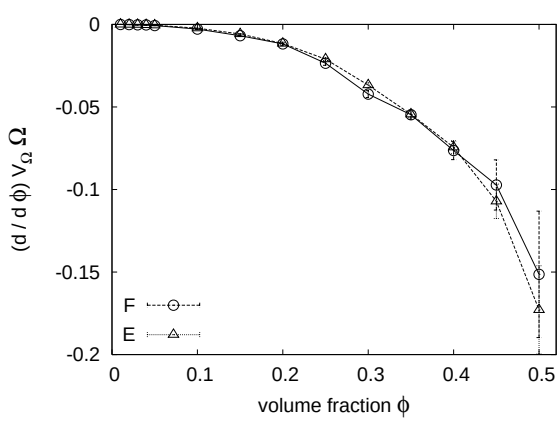

FIG. 12: $\mathrm{d}(V_\Omega\Omega)/\mathrm{d}\phi$ vs. ϕ from Eqs. (61) (circles) and (62) (triangles).

Figure 12 shows $\mathrm{d}(V_\Omega\Omega)/\mathrm{d}\phi$ calculated using the two results for V_3 shown in Fig. 10 and V_1 from Eq. (55). We do not have a dilute-limit value to compare with these results. However they appear to be numerically well-behaved and non-zero.

The computed values of the coefficients of the vector $\boldsymbol{V}$ are shown in Table II.

V. THE AXIAL VECTOR OF THE ANTISYMMETRIC STRESS

The closure relation for the axial vector of the antisymmetric stress $\boldsymbol{R}$ in principle may contain several terms as shown in the Appendix. However, as in the case of the symmetric stress, we are able to calculate the closure coefficient only for the first term:

$$\boldsymbol{R} = R_1\boldsymbol{\Omega}_\Delta. \quad (63)$$

The leading term for the torque problem is k^0 and, equating the corresponding coefficients, gives

$$A^{[R]^0_T} = R_1 A^{[\Omega_\Delta]^0_T}, \quad (64)$$

$$A^{[R]^\parallel_T} = R_1 A^{[\Omega_\Delta]^\parallel_T} + \phi\frac{\mathrm{d}R_1}{\mathrm{d}\phi}A^{[\Omega_\Delta]^0_T}, \quad (65)$$

$$A^{[R]^\perp_T} = R_1 A^{[\Omega_\Delta]^\perp_T} + \phi\frac{\mathrm{d}R_1}{\mathrm{d}\phi}A^{[\Omega_\Delta]^0_T} \quad (66)$$

which are the analog of Eqs. (41) to (45) for this case. Terms of higher-order in k are shown in the Appendix.

From (64), which derives from the constant term of the torque problem, we have

$$R_1(\phi) = \frac{A^{[R]^0_T}}{A^{[\Omega_\Delta]^0_T}} = \frac{3\phi}{\Omega(\phi)}, \quad (67)$$

where use has been made of the fact that $A^{[R]^0_T}$ equals 3ϕ as shown in Ref. 27, and $A^{[\Omega_\Delta]^0_T}$ is $\Omega(\phi)$, the hindrance function for rotation,[29] a graph of which is given in the reference. Figure 13 shows R_1 calculated from this equation. The line is calculated using the following fit for $\Omega(\phi)$:

$$\Omega = 1.0 - 1.5\phi + 0.67\phi^2 \quad (68)$$

When R_1 calculated from (67) is substituted into (65) ($T^\parallel$ term), we have

$$\phi\frac{\mathrm{d}R_1}{\mathrm{d}\phi} = \frac{1}{A^{[\Omega_\Delta]^0_T}}\left(A^{[R]^\parallel_T} - A^{[R]^0_T}\frac{A^{[\Omega_\Delta]^\parallel_T}}{A^{[\Omega_\Delta]^0_T}}\right). \quad (69)$$

while, in a similar way, we find from (66) ($T^\perp$ term)

$$\phi\frac{\mathrm{d}R_1}{\mathrm{d}\phi} = \frac{1}{A^{[\Omega_\Delta]^0_T}}\left(A^{[R]^\perp_T} - A^{[R]^0_T}\frac{A^{[\Omega_\Delta]^\perp_T}}{A^{[\Omega_\Delta]^0_T}}\right). \quad (70)$$

Figure 14 shows $\mathrm{d}R_1/\mathrm{d}\phi$ calculated from (69) and (70)

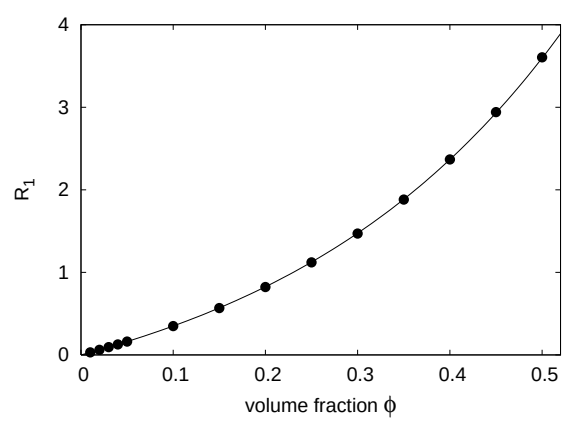

FIG. 13: The coefficient R_1 defined in Eq. (63) calculated from (67).

as well as the derivative of R_1 calculated from the fit mentioned before. The consistency is very good.

TABLE II: Closure coefficients.

ϕ	V_1	V_2	$V_3$from$F$	$V_3$from$E$	$\mathrm{d}(V_\Omega\Omega)/\mathrm{d}\phi$	R_1
0.01	0.00312	0.143	−0.001	−0.0006	−0.00003	0.03045
0.02	0.00654	0.14	−0.002	−0.0017	−0.00008	0.06181
0.03	0.0103	0.15	−0.003	−0.0018	−0.0003	0.09411
0.04	0.0144	0.15	−0.004	−0.003	−0.0003	0.12738
0.05	0.0190	0.15	−0.006	−0.004	−0.0007	0.1617
0.10	0.0489	0.15	−0.012	−0.009	−0.0029	0.3493
0.15	0.095	0.15	−0.019	−0.016	−0.0070	0.5679
0.20	0.166	0.16	−0.025	−0.024	−0.012	0.8227
0.25	0.269	0.15	−0.041	−0.033	−0.024	1.1212
0.30	0.41	0.11	−0.06	−0.05	−0.04	1.470
0.35	0.63	0.10	−0.07	−0.07	−0.05	1.882
0.40	0.94	0.2	−0.09	−0.08	−0.08	2.368
0.45	1.4	0.1	−0.11	−0.13	−0.10	2.94
0.50	2.1	0.0	−0.1	−0.20	−0.2	3.61

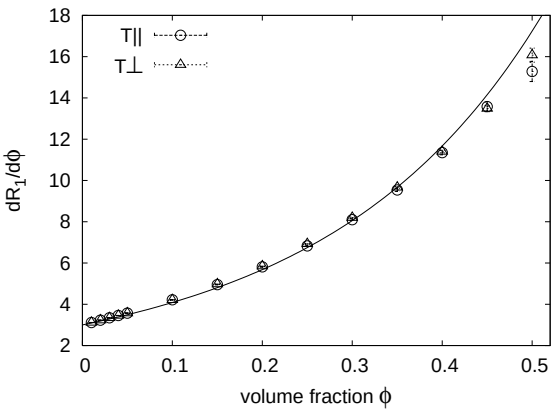

FIG. 14: $dR_1/d\phi$ from (69) (circles) and (70) (triangles); the line is the analytical derivative of a fit to the data.

VI. CONCLUSIONS

Our study of the stress in a spatially non-uniform suspension of equal spheres in Stokes flow has been based on the identification of the three components of this quantity shown in Eq. (1): a symmetric traceless term, and an antisymmetric term consisting of an axial and a polar contribution. This result, derived in Ref. 32 and, more generally, in Ref. 36, extends the well-known result of Batchelor[43] to the non-homogeneous case. The focus of this paper has been on the derivation of closure relations for these quantities.

We have considered three different physical problems: particles subjected to a force, a torque, and shear, finding, for the effective properties that we could test, the same (or, at least numerically consistent) values in all the problems. For example, we were able to find four independent determinations of the effective viscosity μ_e, all of which give very consistent values. We have also found that, to leading order in the spatial dishomogeneity, it is consistent to evaluate μ_e in correspondence of the local volume fraction ϕ, with other possible terms only giving higher-order contributions to the symmetric component of the stress. A similar conclusion was reached for the closure of the axial component of the antisymmetric stress.

The polar component of the antisymmetric stress, $\boldsymbol{V}$, is a new effect which had not been identified before. We have found a closure relation for this quantity, the coefficients of which also exhibit consistency among the different problems. Thus, the existence of this quantity seems well defined beyond any uncertainty deriving from statistical error. For the axial component of the antisymmetric stress, our results are more limited but are in agreement with those found by others.

Due to the imperfectly understood consequences of the artificial periodicity arising from the use of a repeated fundamental cell, we have only been able to focus on the leading-order behavior in the wave number k of the spatial non-uniformity. To this order, we have found that the dominant term of the symmetric stress is the product of the effective viscosity and E_m, the rate of strain of the volumetric flux of the mixture $\boldsymbol{u}_m$. In comparison with this term, the other terms that could possibly be present give contributions lower by an order k^2, which our methods prevent us from determining.

Since it is $\boldsymbol{\nabla}\times\boldsymbol{\nabla}\times\boldsymbol{V}$ which enters the momentum equation, the contribution of $\boldsymbol{V}$ to the momentum equation is also $O(k^2)$ smaller than that of $\boldsymbol{\nabla}\cdot(\mu_e\mathsf{E}_m)$. Thus, at least for the three physical situations studied here, the new term $\boldsymbol{V}$ would only give a small contribution. Whether this conclusion holds generally depends on the relative magnitude of the spatially non-uniform parts of $\boldsymbol{u}_m$ and the slip velocity $\boldsymbol{u}_\Delta$. It does not appear possible to make a general statement about this point at this time.

Our results have been obtained by carrying out ensemble averages using biased probability distributions corresponding to a prescribed form of the particle number density. We have not attempted to incorporate any special structure for the two-particle and higher-order particle

distribution functions which, as is well known, in general depend on the particular flow considered. In a recent paper,[29] we have shown how to bias the probability distribution so as to reproduce an arbitrary functional form for the particle number density. We believe that a similar approach will enable us to control the second- and higher-order distribution functions. This point will be pursued in future publications.

Acknowledgments

We wish to acknowledge the support by DOE grant DE-FG02-99ER14966.

APPENDIX: DETAILS OF THE CLOSURES

1. Expression for the stress

Equation (1) was given as Eq. (10.19) in Ref.[32]. Explicit expressions for the various contributions were derived in terms of the coefficients appearing in Lamb's general solution of the Stokes equations[33–35] in the form

$$\mathsf{S} = \frac{4}{3}\pi\mu\sum_{l=2}^{\infty}\frac{(-1)^{l+1}}{l!}(2l+1)\mathcal{S}_l(a^2\nabla^2)\ \boldsymbol{\nabla}^{l-2}\cdot\left(n\overline{\left[\boldsymbol{\nabla}^l\left(r^{2l+1}q_{-l-1}\right)\right]_{r=a}}\right), \tag{A.1}$$

$$\boldsymbol{R} = \frac{4}{3}\pi\mu\sum_{l=2}^{\infty}\frac{(-1)^{l+1}}{(l-1)!}\left\{(2l+1)\mathcal{S}_l(a^2\nabla^2)\ \boldsymbol{\nabla}^{l-1}\cdot\left(n\overline{\left[\boldsymbol{\nabla}^l\left(r^{2l+1}\chi_{-l-1}\right)\right]_{r=a}}\right)\right\}, \tag{A.2}$$

$$\begin{aligned}\boldsymbol{V} = \frac{4}{3}\pi\mu\sum_{l=2}^{\infty}\frac{(-1)^{l+1}}{l!}&\left\{(2l+1)(2l+3)\mathcal{S}_{l+1}(a^2\nabla^2)\ \boldsymbol{\nabla}^{l-1}\cdot\left(n\overline{\left[\boldsymbol{\nabla}^l\left(r^{2l+1}\phi^*_{-l-1}\right)\right]_{r=a}}\right)\right.\\ &\left.+a^2\mathcal{S}_{l+1}(a^2\nabla^2)\ \boldsymbol{\nabla}^{l-1}\cdot\left(n\overline{\left[\boldsymbol{\nabla}^l\left(r^{2l+1}q_{-l-1}\right)\right]_{r=a}}\right)\right\}.\end{aligned} \tag{A.3}$$

Here the operators $\mathcal{S}_l$ are defined by

$$\mathcal{S}_l = \frac{3}{(2l+1)!!}\left[1+\frac{a^2\nabla^2}{1!2^1(2l+3)}+\frac{(a^2\nabla^2)^2}{2!2^2(2l+3)(2l+5)}+\cdots\right]. \tag{A.4}$$

The term $\left[\boldsymbol{\nabla}^l\left(r^{2l+1}q_{-l-1}\right)\right]_{r=a}$ and similar ones are constants, and the overline denotes the ensemble average.

2. The polar vector of the antisymmetric stress $\boldsymbol{V}$

The closure relation for the polar vector $\boldsymbol{V}$ in terms of $\boldsymbol{u}_m$, $\boldsymbol{u}_\Delta$, and $\boldsymbol{\Omega}_\Delta$ must have the form in (48), where we neglect possible terms containing higher order derivatives. Upon combining the parameterizations for the three different problems into a single expression as in Ref. 29, which is justified by the linearity of the problem, we write:

$$\begin{aligned}\boldsymbol{V}(\boldsymbol{x}) = {}&[V]^0_F\boldsymbol{W}_F\\ &+\epsilon\sin(\boldsymbol{k}\cdot\boldsymbol{x})\left([V]^{\parallel}_F\boldsymbol{W}^{\parallel}_F+[V]^{\perp}_F\boldsymbol{W}^{\perp}_F\right)\\ &+\epsilon\cos(\boldsymbol{k}\cdot\boldsymbol{x})\,[V]^{\perp}_T\boldsymbol{W}^{\perp}_T\\ &+\epsilon\cos(\boldsymbol{k}\cdot\boldsymbol{x})\left([V]^{\parallel}_E\boldsymbol{W}^{\parallel}_E+[V]^{\perp}_E\boldsymbol{W}^{\perp}_E\right),\end{aligned} \tag{A.5}$$

Upon substituting these parameterizations and the corresponding ones for the velocities into (48) and equating the corresponding terms, we find Eqs. (49) to (54) in the text and

$$\begin{aligned}[V]^{\perp}_F = {}&V_1[u_\Delta]^{\perp}_F+\phi\frac{\mathrm{d}V_1}{\mathrm{d}\phi}[u_\Delta]^0_F-V_3k^2[u_m]^{\perp}_F\\ &+V_\Omega k[\Omega_\Delta]^{\perp}_F,\end{aligned} \tag{A.6}$$

$$\begin{aligned}[V]^{\perp}_E = {}&V_1[u_\Delta]^{\perp}_E-V_3k^2[u_m]^{\perp}_E+V_2k\phi\\ &-V_\Omega k[\Omega_\Delta]^{\perp}_E.\end{aligned} \tag{A.7}$$

The ensemble-averaged coefficients of $\boldsymbol{V}$ have the following k-dependence:

$$[V]^0_F = A^{[V]^0_F}, \tag{A.8}$$

$$[V]^{\parallel}_F = A^{[V]^{\parallel}_F}+kB^{[V]^{\parallel}_F}+k^2C^{[V]^{\parallel}_F}, \tag{A.9}$$

$$[V]^{\perp}_F = A^{[V]^{\perp}_F}+kB^{[V]^{\perp}_F}+k^2C^{[V]^{\perp}_F}, \tag{A.10}$$

$$[V]^{\perp}_T = k\left(A^{[V]^{\perp}_T}+kB^{[V]^{\perp}_T}\right), \tag{A.11}$$

$$[V]^{\parallel}_E = k\left(A^{[V]^{\parallel}_E}+kB^{[V]^{\parallel}_E}\right), \tag{A.12}$$

$$[V]^{\perp}_E = k\left(A^{[V]^{\perp}_E}+kB^{[V]^{\perp}_E}\right). \tag{A.13}$$

We now substitute all the k-parameterizations of the various ensemble-averaged coefficients for $\boldsymbol{V}$, $\boldsymbol{u}_m$, etc. into

Eqs. (49) to (54). In this way, at the leading order in k – i.e., $O(k^0)$ in the force problem and $O(k^1)$ in the torque and shear problems – we find Eqs. (55) to (60).

3. The axial vector of the antisymmetric stress $\boldsymbol{R}$

In principle, the closure relation for the axial vector of the antisymmetric stress $\boldsymbol{R}$ must feature the relative angular velocity $\boldsymbol{\Omega}_\Delta$ and the axial vectors that can be constructed with $\boldsymbol{u}_m$ and $\boldsymbol{u}_\Delta$ by taking the curl. The resulting expression then takes the form

$$\begin{aligned}\boldsymbol{R} &= R_1\boldsymbol{\Omega}_\Delta \\ &\quad +R_2a^2\boldsymbol{\nabla}\times(\mathsf{E}_m\cdot\boldsymbol{\nabla}\phi)+R_3a^2\nabla^2\boldsymbol{\nabla}\times\boldsymbol{u}_m \\ &\quad +R_4a^2\boldsymbol{\nabla}\times\boldsymbol{u}_\Delta+R_5\left(\boldsymbol{\nabla}\phi\right)\times\boldsymbol{u}_\Delta. \end{aligned}\tag{A.14}$$

As before, other possible terms containing higher-order derivatives have been neglected.

In this case, the role played before by the fundamental polar vector $\boldsymbol{W}$ for each one of the three problems is played by a fundamental axial vector $\boldsymbol{\omega}$. For the force problem, this is given by

$$a\boldsymbol{\omega}_F^\perp = \hat{\boldsymbol{k}}\times\boldsymbol{W}_F, \tag{A.15}$$

for the torque problem by

$$\boldsymbol{\omega}_T=\frac{\boldsymbol{T}_0}{8\pi\mu a^3}, \tag{A.16}$$

and, for the shear problem, by

$$\boldsymbol{\omega}_F^\perp = \hat{\boldsymbol{k}}\times\left(\mathsf{E}^\infty\cdot\hat{\boldsymbol{k}}\right). \tag{A.17}$$

The equation analogous to (A.5) is

$$\begin{aligned}\boldsymbol{R}(\boldsymbol{x}) &= [R]_T^0\boldsymbol{\omega}_T \\ &+ \epsilon\cos\left(\boldsymbol{k}\cdot\boldsymbol{x}\right)[R]_F^\perp\boldsymbol{\omega}_F^\perp \\ &+ \epsilon\sin\left(\boldsymbol{k}\cdot\boldsymbol{x}\right)\left([R]_T^\parallel\boldsymbol{\omega}_T^\parallel+[R]_T^\perp\boldsymbol{\omega}_T^\perp\right) \\ &+ \epsilon\sin\left(\boldsymbol{k}\cdot\boldsymbol{x}\right)[R]_E^\perp\boldsymbol{\omega}_E^\perp, \end{aligned}\tag{A.18}$$

in which $\boldsymbol{\omega}_T^\parallel$ and $\boldsymbol{\omega}_T^\perp$ are the components of $\boldsymbol{\omega}_T$ parallel and perpendicular to $\boldsymbol{k}$. As before we find

$$[R]_T^0 = R_1[\Omega_\Delta]_T^0, \tag{A.19}$$

$$[R]_T^\parallel = R_1[\Omega_\Delta]_T^\parallel+\phi\frac{\mathrm{d}R_1}{\mathrm{d}\phi}[\Omega_\Delta]_T^0, \tag{A.20}$$

$$\begin{aligned}[R]_T^\perp &= R_1[\Omega_\Delta]_T^\perp+\phi\frac{\mathrm{d}R_1}{\mathrm{d}\phi}[\Omega_\Delta]_T^0 \\ &\quad +R_3k^3[u_m]_T^\perp-R_4k[u_\Delta]_T^\perp, \end{aligned}\tag{A.21}$$

$$\begin{aligned}[R]_F^\perp &= R_1[\Omega_\Delta]_F^\perp \\ &\quad -R_3k^3[u_m]_F^\perp+R_4k[u_\Delta]_F^\perp \\ &\quad +R_5\phi k[u_\Delta]_F^0, \end{aligned}\tag{A.22}$$

$$\begin{aligned}[R]_E^\perp &= -\frac{R_3}{2}k[u_m]_E^\perp+R_1[\Omega_\Delta]_E^\perp \\ &\quad +R_3k^3[u_m]_E^\perp-R_4k[u_\Delta]_E^\perp \\ &\quad -R_2k^2\phi. \end{aligned}\tag{A.23}$$

The k-dependence fit for the coefficients of $\boldsymbol{R}$ is

$$[R]_T^0 = A^{[R]_T^0}, \tag{A.24}$$

$$[R]_T^\parallel = A^{[R]_T^\parallel}+k^2C^{[R]_T^\parallel}, \tag{A.25}$$

$$[R]_T^\perp = A^{[R]_T^\perp}+k^2C^{[R]_T^\perp}, \tag{A.26}$$

$$[R]_F^\perp = k\left(A^{[R]_F^\perp}+kB^{[R]_F^\perp}\right), \tag{A.27}$$

$$[R]_E^\perp = k^2\left(A^{[R]_E^\perp}+kB^{[R]_E^\perp}\right) \tag{A.28}$$

from which, by the usual procedure, we derive Eqs. (64), (65), and (66) to the leading order $O(k^0)$.

4. k-expansions of the average coefficients for $\boldsymbol{\Omega}$, $\boldsymbol{u}_m$, and $\boldsymbol{u}_\Delta$

Here we summarize the k-expansions of the averages for $\boldsymbol{\Omega}_\Delta$, $\boldsymbol{u}_\Delta$, and $\boldsymbol{u}_m$, which were given in our earlier paper.[29]

$$[\Omega_\Delta]_T^0 = A^{[\Omega_\Delta]_T^0}, \tag{A.29}$$

$$[\Omega_\Delta]_T^\parallel = A^{[\Omega_\Delta]_T^\parallel}+(ka)^2C^{[\Omega_\Delta]_T^\parallel}, \tag{A.30}$$

$$[\Omega_\Delta]_T^\perp = A^{[\Omega_\Delta]_T^\perp}+(ka)^2C^{[\Omega_\Delta]_T^\perp}, \tag{A.31}$$

$$[\Omega_\Delta]_F^\perp = (ka)\left(A^{[\Omega_\Delta]_F^\perp}+(ka)B^{[\Omega_\Delta]_F^\perp}\right), \tag{A.32}$$

$$[\Omega_\Delta]_E^\perp = (ka)^2A^{[\Omega_\Delta]_E^\perp}, \tag{A.33}$$

$$\begin{aligned}[u_m]_F^\perp &= \frac{1}{(ka)^2}\left(D^{[u_m]_F^\perp}+(ka)^2A^{[u_m]_F^\perp}\right. \\ &\qquad \left.+(ka)^3B^{[u_m]_F^\perp}\right), \end{aligned}\tag{A.34}$$

$$[u_m]_T^\perp = \frac{1}{ka}\left(D^{[u_m]_T^\perp}+(ka)^2A^{[u_m]_T^\perp}\right), \tag{A.35}$$

$$[u_m]_E^\perp = \frac{1}{ka}\left(D^{[u_m]_E^\perp}+(ka)^2A^{[u_m]_E^\perp}\right), \tag{A.36}$$

$$[u_\Delta]_F^0 = A^{[u_\Delta]_F^0}+(ka)B^{[u_\Delta]_F^0}, \tag{A.37}$$

$$[u_\Delta]_F^\parallel = A^{[u_\Delta]_F^\parallel}+(ka)B^{[u_\Delta]_F^\parallel}, \tag{A.38}$$

$$[u_\Delta]_F^\perp = A^{[u_\Delta]_F^\perp}+(ka)B^{[u_\Delta]_F^\perp}, \tag{A.39}$$

$$[u_\Delta]_T^\perp = (ka)\left(A^{[u_\Delta]_T^\perp}+(ka)B^{[u_\Delta]_T^\perp}\right), \tag{A.40}$$

$$[u_\Delta]_E^\parallel = (ka)\left(A^{[u_\Delta]_E^\parallel}+(ka)B^{[u_\Delta]_E^\parallel}\right), \tag{A.41}$$

$$[u_\Delta]_E^\perp = (ka)\left(A^{[u_\Delta]_E^\perp}+(ka)B^{[u_\Delta]_E^\perp}\right). \tag{A.42}$$

* Electronic address: ichiki@mailaps.org
† Electronic address: prosperetti@jhu.edu

[1] M. Ishii, *Thermo-Fluid Dynamic Theory of Two-Phase Flow* (Eyrolles, Paris, 1975).
[2] D. A. Drew, "Mathematical modeling of two-phase flow," Ann. Rev. Fluid Mech. **15**, 261 (1983).
[3] D. D. Joseph and T. S. Lundgren, "Ensemble averaged and mixture theory equations for incompressible fluid-particle suspensions," Int. J. Multiphase Flow **16**, 35 (1990).
[4] A. Prosperetti, "Some considerations on the modeling of disperse multiphase flows by averaged equations," JSME Int. J. **B42**, 573 (2000).
[5] T. B. Anderson and R. Jackson, "A fluid mechanical description of fluidized beds," I & EC Fundamentals **6**, 527 (1967).
[6] S. Sundaresan, "Instabilities in fluidized beds," Ann. Rev. Fluid Mech. **35**, 63 (2003).
[7] D. L. Koch, "Kinetic theory for a monodisperse gas-solid suspension," Phys. Fluids **A2**, 1711 (1990).
[8] H. K. Tsao and D. L. Koch, "Simple shear flows of dilute gas-solid suspensions," J. Fluid Mech. **296**, 211 (1995).
[9] A. S. Sangani, G. B. Mo, H. K. Tsao, and D. L. Koch, "Simple shear flow of dense gas-solid suspensions at finite Stokes numbers," J. Fluid Mech. **313**, 309 (1996).
[10] S. Y. Kang, A. S. Sangani, H. K. Tsao, and D. L. Koch, "Rheology of dense bubble suspensions," Phys. Fluids **9**, 1540 (1997).
[11] D. L. Koch and A. S. Sangani, "Particle pressure and marginal stability limits for a homogeneous monodisperse gas-fluidized bed: kinetic theory and numerical simulations," J. Fluid Mech. **400**, 229 (1999).
[12] R. J. Phillips, R. C. Armstrong, and R. A. Brown, "A constitutive equation for concentrated suspensions that accounts for the shear-induced particle migration," Phys. Fluids **A4**, 30 (1992).
[13] J. F. Brady and J. F. Morris, "Microstructure of strongly sheared suspensions and its impact on rheology and diffusion," J. Fluid Mech. **348**, 103 (1997).
[14] J. Bergenholtz, J. F. Brady, and M. Vicic, "The non-Newtonian rheology of dilute colloidal suspensions," J. Fluid Mech. **456**, 239 (2002).
[15] J. F. Brady, "The rheological behavior of concentrated colloidal dispersions," J. Chem. Phys. **99**, 567 (1993).
[16] D. L. Koch and A. J. C. Ladd, "Moderate Reynolds number flow through periodic and random arrays of aligned cylinders," J. Fluid Mech. **349**, 31 (1997).
[17] N. A. Patankar, D. D. Joseph, J. Wang, R. D. Barree, M. Conway, and M. Asadi, "Power law correlations for sediment transport in pressure driven channel flows," Int. J. Multiphase Flow **28**, 1269 (2002).
[18] A. Biesheuvel and S. Spoelstra, "The added mass coefficient of a dispersion of spherical gas bubbles in liquid," Int. J. Multiphase Flow **15**, 911 (1989).
[19] A. S. Sangani and A. K. Didwania, "Dispersed-phase stress tensor in flows of bubbly liquids at large Reynolds numbers," J. Fluid Mech. **248**, 27 (1993).
[20] D. Z. Zhang and A. Prosperetti, "Averaged equations for inviscid disperse two-phase flow," J. Fluid Mech. **267**, 185 (1994).
[21] P. D. M. Spelt and A. S. Sangani, "Properties and averaged equations for flows of bubbly liquids," Appl. Sci. Res. **58**, 337 (1997/1998).
[22] J. F. Brady and G. Bossis, "Stokesian dynamics," Ann. Rev. Fluid Mech. **20**, 111 (1988).
[23] C. C. Chang and R. L. Powell, "The rheology of bimodal hard-sphere dispersions," Phys. Fluids **6**, 1628 (1994).
[24] C. K. Aidun, Y. Lu, and E.-J. Ding, "Direct analysis of particulate suspensions with inertia using the discrete Boltzmann equation," J. Fluid Mech. **37**, 287 (1998).
[25] M. Marchioro and A. Acrivos, "Shear-induced particle diffusivities from numerical simulations," J. Fluid Mech. **443**, 101 (2001).
[26] M. Marchioro, M. Tanksley, and A. Prosperetti, "Flow of spatially non-uniform suspensions. Part I: Phenomenology," Int. J. Multiphase Flow **26**, 783 (2000).
[27] M. Marchioro, M. Tanksley, W. Wang, and A. Prosperetti, "Flow of spatially non-uniform suspensions. Part II: Systematic derivation of closure relations," Int. J. Multiphase Flow **27**, 237 (2001).
[28] W. Wang and A. Prosperetti, "Flow of spatially non-uniform suspensions. Part III: Closure relations for porous media and spinning particles," Int. J. Multiphase Flow **27**, 1627 (2001).
[29] K. Ichiki and A. Prosperetti, "Faxén-like relations for a non-uniform suspension," Phys. Fluids (2004). (accepted)
[30] Q. Zhang, K. Ichiki, and A. Prosperetti, "Esnemble averaging for spatially non-uniform systems," Phys. Rev. E. (in preparation)
[31] R. A. Lionberger and W. B. Russel, "Microscopic theories of the rheology of stable colloidal dispersions," Adv. Chem. Phys. **111**, 399 (2000).
[32] M. Tanksley and A. Prosperetti, "Average pressure and velocity fields in non-uniform suspensions of spheres in Stokes flow," J. Eng. Math. **41**, 275 (2001).
[33] H. Lamb, *Hydrodynamics*, 6th ed. (Cambridge U.P., Cambridge, 1932).
[34] J. Happel and H. Brenner, *Low-Reynolds Number Hydrodynamics* (Prentice-Hall, Englewood Cliffs, 1965).
[35] S. Kim and S. J. Karrila, *Microhydrodynamics* (Butterworth-Heinemann, Boston, 1991).
[36] A. Prosperetti, "The average stress in incompressible disperse flow, *Int. J. Multiphase Flow*," Int. J. Multiphase Flow (2004). (submitted)
[37] L. D. Landau and E. M. Lifshitz, *Fluid Mechanics* (Pergamon, Oxford, 1959).
[38] C. W. J. Beenakker, "The effective viscosity of a concentrated suspension of spheres (and its relation to diffusion)," Physica **128A**, 48 (1984).
[39] D. R. Foss and J. F. Brady, "Structure, diffusion and rheology of Brownian suspensions by Stokesian Dynamics simulation," J. Fluid Mech. **407**, 167 (2000).
[40] G. K. Batchelor and J. T. Green, "The hydrodynamic interaction of two small freely-moving spheres in a linear flow field," J. Fluid Mech. **56**, 375 (1972).
[41] A. J. C. Ladd, "Hydrodynamic transport coefficients of random dispersions of hard spheres," J. Chem. Phys. **93**, 3484 (1990).
[42] K. C. Nunan and J. B. Keller, "Effective viscosity of a periodic suspension," J. Fluid Mech. **142**, 269 (1984).
[43] G. K. Batchelor, "The stress system in a suspension of force-free particles," J. Fluid Mech. **41**, 545 (1970).